ELSEVIER

Chemical Engineering Journal 85 (2002) 327–338

Chemical Engineering Journal

www.elsevier.com/locate/cej

Kinetics of *p*-nitrophenol degradation: effect of reaction conditions and cavitational parameters for a multiple frequency system

Manickam Sivakumar, Prashant A. Tatake, Aniruddha B. Pandit*

Chemical Engineering Division, University Department of Chemical Technology (UDCT), University of Mumbai, Matunga, Mumbai 400019, India

Received 26 January 2001; accepted 25 May 2001

Abstract

In order to assess the ultrasound dual frequency effects, sonochemical degradation of *p*-nitrophenol (*p*-NP) in an aqueous solution has been carried out with ultrasound at three operating frequencies, i.e., at 25, 40 kHz each independently, and the combination of two frequencies (25 + 40 kHz) simultaneously. Based on the rates of degradation, a kinetic study has been performed which leads to the evaluation of apparent kinetic rate constants for the degradation of *p*-NP. The influence of various parameters including initial solution pH, bulk solution temperature, on the degradation of *p*-NP was studied for these three frequency modes (25, 40 and 25 + 40 kHz) in order to investigate the temporal behaviour of this reaction, especially when it was operated in combined mode (25 + 40 kHz). The energy efficiency in the case of dual frequency mode is much better than single frequency modes. Modelling and cavity dynamics simulations have also been carried out to explain the observed effects. During combined mode operation, an improvement in the rate of degradation has been observed. The variation in the rate constants has been explained based on the difference in the acoustic pressure field in different systems including ultrasonic bath and dual frequency processor.

Keywords: Ultrasonic wave; Sonolysis; *p*-NP; Frequency effects; 25, 40 and 25 + 40 kHz

1. Introduction

The chemical effects of ultrasonic irradiation were first reported more than 70 years ago. However, very few studies have been focused on the detailed kinetics and mechanisms of chemical reactions in the presence of ultrasound [1]. Ultrasound has been used to induce or accelerate a variety of reactions. Ultrasound is responsible for high-energy chemical reactions in liquids, principally due to acoustic cavitation—the formation, growth and implosive collapse of bubbles [2]. The growth and collapse of these bubbles then resulting into transfer and focusing of energy from the macroscale vibratory motion of the acoustic transducer to the vapour inside the bubbles. The bubble collapse produces intense local heating and high pressures for a short lifetime of a few nanoseconds. Theoretical models based on Rayleigh–Plesset equation predict that during the collapse, high temperatures and pressures exceeding the critical values of water (temperature of 647 K and pressure of 22.4 MPa) occur in the liquid phase [3]. Thus, cavitation serves as a means of concentrating the diffused energy of sound into microreactors [2]. Even though the local temperature and pressure conditions created by the cavity implosion are extreme, one can have good control over the sonochemical reactions. The intensity of cavity implosion, and hence the nature of the reaction, are controlled by factors such as driving acoustic frequency, acoustic intensity, bulk temperature, static pressure, the choice of the liquid, and the choice of the dissolved gas [2]. The heat from the cavity implosion decomposes water into extremely reactive hydrogen atoms ($H^{\bullet}$) and hydroxyl radicals ($OH^{\bullet}$). During the quick-cooling phase, hydroxyl radicals and hydrogen atoms recombine to form hydrogen peroxide (H_2O_2) and molecular hydrogen (H_2), respectively. Thus, in such a molecular environment, organic compounds and inorganic compounds are oxidised or reduced depending on their reactivity.

Although ultrasound has a broad range of industrial applications, its potential for water and wastewater treatment has not been explored extensively [4]. Increasingly stringent water quality regulations require almost total removal of organic pollutants from effluent wastewater from a level of part-per-million to part-per-billion range. The efficiency of the usual cleaning processes to treat carbonaceous compounds (biological or physical/chemical treatments) is limited. For example, biological treatments are uneconomical for the effluent waste, which is highly concentrated. Air stripping treatment is, rather, a pollution shift. Adsorption

* Corresponding author. Tel.: +91-22-4145616; fax: +91-22-4145614.
E-mail address: abp@udct.ernet.in (A.B. Pandit).

1385-8947/02/$ – see front matter
PII: S1385-8947(01)00179-6

Nomenclature

C	velocity of sound (m/s)
dR/dt	bubble wall velocity (m/s)
d^2R/dt^2	bubble wall acceleration (m/s^2)
E	energy required to expand a population of bubbles (J)
f	frequency of ultrasound (kHz)
I	intensity of ultrasound (W/m^2)
N	number of bubbles in solution (–)
P	magnitude of the hydrostatic and acoustic pressure (N/m^2)
P_A	peak positive pressure amplitude (N/m^2)
P_i	pressure inside the bubble at time t (N/m^2)
P_t	time-dependent instantaneous pressure (N/m^2)
P_v	vapour pressure (N/m^2)
P_0	initial pressure inside the bubble (N/m^2)
P_∞	pressure in the surrounding liquid (N/m^2)
R	radius of the bubble at time t (μm)
R_c	radius of the bubble at collapse (μm)
R_m	maximum radius of the bubble (μm)
R_m^3/t_c	(m^3/s)
R_0	initial radius of the bubble (μm)
t	time (s)
t_c	collapse time of the cavity (s)

Greek letters

λ	wavelength of ultrasound (m^{-1})
μ	viscosity (Pa s)
ρ_1	density of liquid (kg/m^3)
σ	surface tension (N/m^2)
ϕ	phase difference between the two waves (–)

on granulated activated carbon or filtration on membranes needs a subsequent incineration. Thermal treatment leads to incomplete combustion and products that are often as toxic as the initial pollutants can be formed. In such circumstances, ultrasound seems to be a promising technology for wastewater treatment.

There are two mechanisms responsible for the oxidation/degradation of organic pollutants, again, which is decided on the basis of physical and chemical properties of the pollutants. The first mechanism is pyrolysis and is expected to be the main reaction path for the degradation of hydrophobic or apolar and more volatile compounds, which enter and decompose inside the cavitation bubbles in the form of vapour. The second mechanism is the generation of hydroxyl radicals in the cavitation bubbles, which subsequently are thrown out in the bulk liquid on cavity collapse and oxidise the organic compounds which are hydrophilic or polar and non-volatile compounds, present near the interface of the cavity–liquid. Still, pyrolysis also occurs when polar compounds are sonicated. Currell et al. [5] found that the sonication of phenol yields acetylene as well, which is possible only under pyrolytic conditions.

Even though, oxidation/degradation is affected by various parameters of ultrasound such as frequency and intensity of the sound wave, the most important and controllable parameter is frequency, since it has varied effects on the bubble dynamics resulting into different temperature and pressure conditions at collapse and hence the rate of the reaction under the given conditions. Conventionally, only waves of single frequency are used in a given system. Interestingly, there is also a way of subjecting a given solution with two different frequencies simultaneously. Such an arrangement makes the emitting waves of two different frequencies to undergo interference of constructive nature based on the superposition principle. As a result of this, the amplitude of the resultant wave is larger than the two individual waves emitted from two different frequency sources due to the reverberation of ultrasound. This results in higher cavity growth and ultimately causing more intense cavitational collapse. Thus, applying two frequencies, results in excitation of greater number of bubbles in a given cavity/bubble population. Simulations indicate that for a cavity to attain the same maximum size during its growth, the amount of energy required for a single sound source is twice the energy associated with the dual frequency processor [6]. Again, the resultant effect of interference of two waves, whether it is constructive or destructive depends on the distance (gapwidth) between the two plates carrying the two different frequency transducers.

High intensity flat plate reverberatory sonicator or the nearfield acoustical processor (NAP) is one such system working on the above principle. It has been used on a larger scale for the extraction of oil from oil shale in a continuous flow operation. Hua et al. [3] have used such a set-up with 16 and 20 kHz frequency magnetostrictive transducers to study the degradation of *p*-nitrophenol (*p*-NP) on a larger scale in continuous flow operation (with the flow rates of 3.2 l min^{-1}). Thoma et al. [7] have also used a similar system for the destruction of dichloromethane and *o*-dichlorobenzene. It is very clear from the above study that such a technology appears to be an alternative for treating large-scale waste effluent in the near future. Also, simulations indicate that such a combination is more energy efficient as discussed earlier. The main focal point here is to find out the parameters involved in the design of such an efficient dual frequency reactor. One such parameter is to determine the critical distance between the two plates (gapwidth) facing each other. These plates are mounted with the transducers of two different frequencies. This parameter has a higher influence as it decides about the length of the cavitation zone or the percentage fraction of the cavitationally active volume generated in a given reactor. It has been well established from the work of Hua et al. [3] that the distance between the plates should be as minimum as possible. This ensures that all of the reactant solution is subjected to ultrasound, resulting in more even dispersal of energy, which is not possible in a conventional probe or a batch reactor due to

the generation of standing waves. Also, attenuation of sound is minimum in such a dual frequency reactor system [3].

Taking advantage of all these factors, our study in detail concentrates on varied parameters, which control the overall reaction using a dual frequency set-up. As a model reaction, degradation of *p*-NP, an industrial water pollutant has been studied in this system using frequencies, namely 25 and 40 kHz by operating them individually as well as in a combined mode; in an attempt to understand and quantify the individual as well as combined frequency effects. These two frequencies were selected based on bubble dynamics modelling. For modelling two sets of frequencies were selected. One set of combination is ranging from 16 to 40 kHz with an increment of 4 kHz in the second wave starting from 16 kHz. Whereas, the second set consists of 25–40 kHz with an increment of 5 kHz in the second wave. From these studies, it was observed that the maximum size of the bubble reached by the 25–40 kHz combination is more as compared to any other combination. This has led us to design a dual frequency reactor with these frequency combinations. A physical cavity dynamics model based on Rayleigh–Plesset equation is also developed to explain the experimentally observed effects.

p-NP has been selected in this study since it is widely used in many industrial processes, as synthetic intermediate or as a raw material in the manufacturing of pesticides, insecticides, wood preservatives, and so forth. Also, it is formed as a by-product during the manufacture of a pesticide parathion. Thus, it is considered to be one of the industrial pollutants and poses a threat to human health. Therefore, it is necessary to develop effective methods for their removal from water, or to reduce them to less harmful intermediates or complete mineralisation.

Kotronarou et al. [1] studied in detail the sonolytic degradation of *p*-NP in aqueous solution using a horn system of 20 kHz and found out the formation of NO^{2-}, NO^{3-} and H^+ as primary products and $HCOO^-$, $C_2O_4{}^{2-}$, and H_2O_2 as secondary products. Their study also involves in detail the effect of pH and the effect of initial concentration of *p*-NP on the degradation kinetics. They have found out that there is a linear increase in the concentration of H_2O_2 during the sonolysis of aqueous *p*-NP solution. The relative faster degradation of *p*-NP have been explained on the basis of thermal decomposition of *p*-NP in the near vicinity region of the hot collapsing gaseous cavities. Based on the products observed they have interpreted an elaborate model involving both $OH^\bullet$ attack and pyrolytic reactions.

2. Experimental

p-NP was obtained from S.D. Finechem, India and it was of at least 99% purity, and used without further purification. Distilled water was used to make-up the solution to the required strength. The initial solution pH values at desired levels were made with NaOH or H_2SO_4 solutions and the change in pH was monitored continuously during the course of the reaction. Absorption spectra were measured with a Chemito-2500 UV–Vis spectrophotometer to monitor the concentration of *p*-NP.

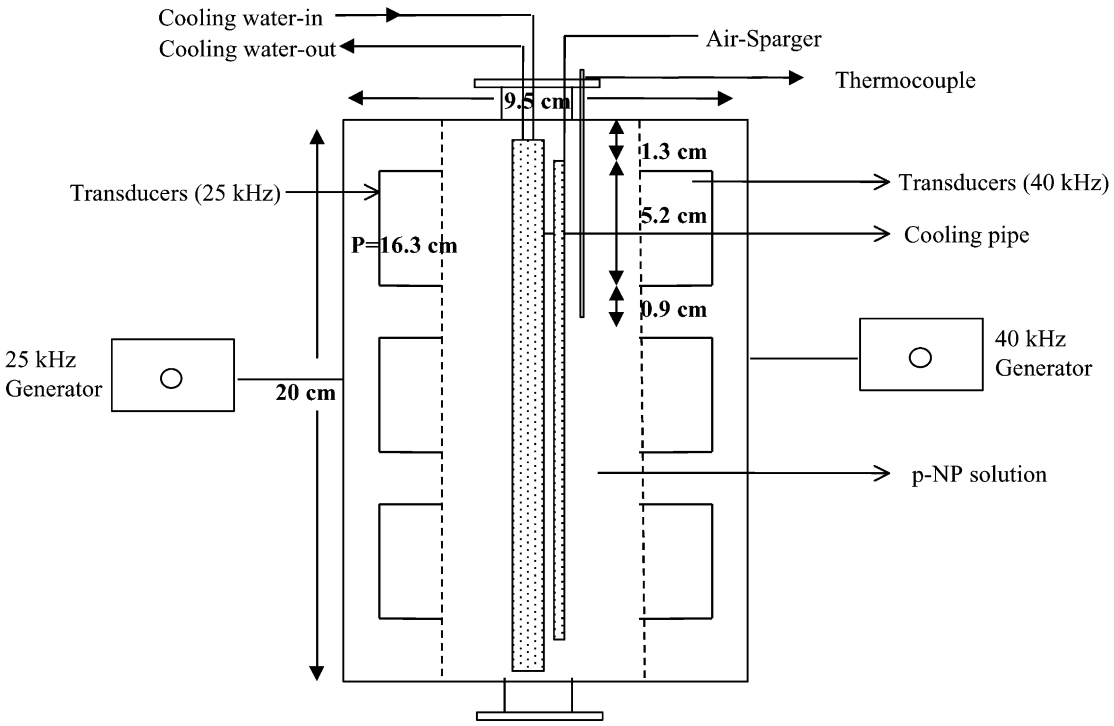

Fig. 1. Schematic representation of dual frequency processor.

The reactions were carried out in a dual frequency acoustic batch reactor, as shown in Fig. 1, which was made entirely of stainless steel with a breadth of 9.5 cm, a depth of 7 cm and a height of 20 cm. The two flattened sides of the reactor were mounted with piezoelectric transducers (3 No. each) driven at 25 and 40 kHz, which were arranged in series, each transducer having a diameter of 5.1 cm. The emitting system was connected to a frequency generator and a power supply. The effective volume of the reactor was 1.5 l. A cooling coil was kept inside the reactor and cold water was pumped from a thermostatic bath in order to maintain the temperature at the selected value within $\pm 2\,^{\circ}C$. The presence of this coil may disturb the nature of the pressure field generated due to a phenomenon called scattering. But, as the coil is present in all the cases of experiments, relative performance still be compared. *p*-NP solution of known concentration of 1.5 l in volume was prepared each time with the required pH and transferred to the reactor. The solution was saturated by sparging with air before and also during the reaction, unless otherwise mentioned. The reactor was also provided with inlet for temperature measurement and outlet for the withdrawal of the samples (it was verified that air alone does not oxidise *p*-NP). Samples were withdrawn from the reactor at regular time interval of 30 min and the concentration of *p*-NP was measured by analysing alkaline solution of these samples in UV at $\lambda = 401$ nm. Typical reaction runs lasted 2.5 h. The calibration curve for *p*-NP was determined using different known concentrations of *p*-NP. Even though application of ultrasound on *p*-NP results in various primary and secondary products as reported by Kotronarou et al. [1], we have restricted our analysis of measuring the concentration of *p*-NP, since the focus was on the frequency effects on the rate of degradation of *p*-NP. In addition to this dual frequency set-up, a horn (Dakshin, 22.5 kHz) with varying tip areas and a bath (Dakshin, 22.5 kHz) were also used in order to have a comparison between these equipments on the degradation rates, based on the efficiency and the nature of the acoustic field generated in each of these equipments. The physical dimensions and characteristics of this dual frequency set-up, ultrasonic horn and ultrasonic bath have been summarised in Table 1.

3. Results of the calorimetry measurements

Calorimetry was used to estimate the electro-acoustic or energy transfer efficiency of the transducer to the solution. Based on the calorimetry experiments, the transfer efficiency of the ultrasonic energy from the transducer to the reactor solution was estimated as 54% for 25 kHz and 42.38% for 40 kHz, whereas for 25 + 40 kHz combined operation it was 45.06% with an assumption that all ultrasonic energy was converted to heat in the reactor. Results of the calorimetry experiments for dual frequency reactor, ultrasonic horn and ultrasonic bath have been tabulated in Table 2. Cavity dynamics was then studied based on the measured power input.

4. Cavity dynamics for a dual frequency acoustic processor

4.1. Modelling of the acoustic pressure field

In the case of multiple transducer systems, the nature of the acoustic field generated is not uniform. Thus, in such systems, it is very important to know whether the transducers are driven (1) perfectly in phase (2) with a constant phase difference or (3) independently. For a dual frequency acoustic field comprising of two frequencies f_1, and f_2, the pressure amplitude for each frequency can be given as

$$P_{A1} = P_0 - P_A(\sin 2\pi f_1 t) \quad (1)$$

$$P_{A2} = P_0 - P_A(\sin 2\pi f_2 t) \quad (2)$$

where P_0 is the ambient pressure, and P_A the pressure amplitude due to the intensity given as

$$P_A = \sqrt{2I\rho_l C} \quad (3)$$

where I is the intensity of the ultrasound (W/m^2), ρ the density of the medium (kg/m^3), and C the velocity of sound in that medium (m/s).

Table 1
Physical dimensions of dual frequency processor, ultrasonic horn and ultrasonic bath

Equipment	Diameter of the emitter (cm)	Total area of dissipation (cm^2)	Sonication volume (ml)
Dual frequency processor			
25 kHz	5.1 (of 3 Nos.)	140	1500
40 kHz	5.1 (of 3 Nos.)	140	1500
25 + 40 kHz	5.1 (of 6 Nos.)	280	1500
Ultrasonic horn			
22.5 kHz	2.5	4.91	100
	2.1	3.46	100
	1.4	1.54	100
Ultrasonic bath			
22.5 kHz	–	225	500

Table 2
Results of calorimetry studies of dual frequency processor, ultrasonic horn and ultrasonic bath

Equipment	Power input (W)	Power input (measured calorimetrically)	Power density (W/cm^3)	Power intensity (W/cm^2)
Dual frequency processor				
25 kHz	120	64.8	0.043	0.46
40 kHz	120	50.85	0.034	0.36
25 + 40 kHz	240	108.15	0.072	0.39
Ultrasonic horn (22.5 kHz)				
Tip area = 4.91 cm^2	240	21.15	0.212	4.31
Tip area = 3.46 cm^2	240	18.25	0.183	5.27
Tip area = 1.54 cm^2	240	12.2	0.122	7.93
Ultrasonic bath				
22.5 kHz	120	40.8	0.082	0.18

Now, considering a phase difference of ϕ, the resultant time-dependent pressure is thus given by

$$P_t = P_0 - P_A[\sin(2\pi f_1 t) + \sin(2\pi f_2 t + \phi)] \quad (4)$$

when $\phi = \pi/2$, the equation gets modified to

$$P_t = P_0 - P_A[\sin(2\pi f_1 t) + \cos(2\pi f_2 t)] \quad (4a)$$

This is one of the possible combinations due to the phase difference between the two sound waves. Here, we have simulated for four such combinations for the two, same or different frequencies. The different combinations taken here are: sin–cos, cos–sin, sin–sin, cos–cos depending upon the phase difference of $\pi/2$ or zero. The results indicate that the maximum size attained by the cavity is more for the case of sin–sin as compared to other three combinations. This is due to the variation in the resultant amplitude, which results in a change in cavity dynamics. Due to this reason, we have considered only the equation

$$P_t = P_0 - P_A[\sin(2\pi f_1 t) + \sin(2\pi f_2 t)] \quad (4b)$$

4.2. Modelling of cavity dynamics

The radial wall motion of the cavity can be described by the cavity dynamics equation developed by Rayleigh and later modified by Plesset, more commonly known as the Rayleigh–Plesset equation [8], and is given as

$$R\left(\frac{d^2R}{dt^2}\right) + \frac{3}{2}\left(\frac{dR}{dt}\right)^2 = \frac{1}{\rho_l}\left[P_i - \frac{4\mu}{R}\left(\frac{dR}{dt}\right) - \frac{2\sigma}{R} - P_\infty\right] \quad (5)$$

where R is the radius of the bubble at time t, P_i the pressure inside the bubble at time t, and P_∞ the pressure in the surrounding liquid.

Therefore for dual frequency

$$P_\infty = P_t = P_0 - P_A[\sin(2\pi f_1 t) + \sin(2\pi f_2 t)] \quad (6)$$

This is a second-order non-linear differential equation which can be solved by fourth-order Runge–Kutta method to find the radius and pressure pulse history of bubble oscillation. This equation is valid up to a point where the bubble wall velocity (dR/dt) is less than the sonic velocity in the cavitating media (in this case water in which $C = 1500\,m/s$). In order to study the effect of an oscillating field on bubble behaviour we can substitute P_t as P_∞ in the above equation.

The simulations were performed using the above equation and the cavity dynamics studied for an initial cavity size of 2 μm (typically that reported in the literature) [9]. The other parameters such as frequency, intensity and temperature were taken at the actual experimental conditions.

5. Results and discussion

5.1. Effect of solution pH

Solution pH is an important factor in determining the physical and chemical properties of the solution, which in turn affects the bubble dynamics. Many researchers [1,5,10,11] have found that the decomposition rate by sonolysis decreased with an increasing solution pH values, while other researchers [12] obtained different results where the decomposition was more rapid in alkaline solutions.

The experimental results of the first-order degradation of *p*-NP by using this set-up at a pH level of 5.0 for the three frequency modes are shown in Fig. 2. In all the pH ranges studied, i.e., pH 3.0, 5.0 and 7.0, the decomposition efficiencies were found to decrease or were constant in some cases with increasing solution pH for a given frequency over the range of pH values used in this study. This suggests that relatively longer times will be required for experiments carried out at higher pH conditions even though the degradation is exponential with respect to time at all pH levels. Fig. 3 shows the effect of pH on the rate constant for the three frequency modes. From this figure it is clear that the apparent rate constant decreased from $k_{3.0} = 1.5 \times 10^{-5}\,s^{-1}$ at pH = 3.0 to $k_{5.0} = 1.33 \times 10^{-5}\,s^{-1}$ at pH = 5.0 and to $k_{7.0} = 1.17 \times 10^{-5}\,s^{-1}$ when the pH was finally increased to 7.0 for 25 kHz frequency. But, for 40 kHz frequency, there was no change in the rate constant for the pH of 3.0 and 5.0,

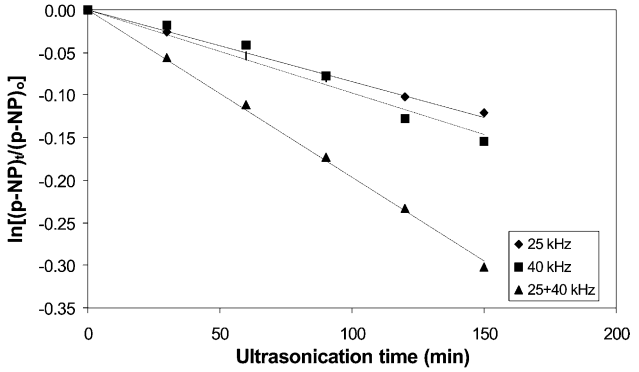

Fig. 2. First-order plot of *p*-NP degradation for three frequency modes at pH 5.0 (20 °C, $C_0 \sim 10$ ppm).

i.e., $k_{3.0} = k_{5.0} = 1.67 \times 10^{-5}\,s^{-1}$. But, for the pH 7.0 it decreased to a value, i.e., $k_{7.0} = 1.5 \times 10^{-5}\,s^{-1}$. In the case of combined mode operation (25 + 40 kHz), the rate constant was $k_{3.0} = 3.50 \times 10^{-5}\,s^{-1}$ at pH 3.0 which marginally decreased and then reached to a constant value during a further increase in pH, i.e., $k_{5.0} = k_{7.0} = 3.33 \times 10^{-5}\,s^{-1}$ at pH 5.0 and 7.0. Thus, for any selected pH, application of 25 + 40 kHz mode gives higher rate constant, followed by 40 and then 25 kHz. Also, for any given operating frequency mode, lowering the pH increases the sonication efficiency or results in higher rate constants. This is due to the fact that with a decrease in pH (higher acid concentration), there is domination of the molecular form of *p*-NP. This molecular form of *p*-NP makes it possible to diffuse into the reactive zone (gas–liquid film region). Also, a small fraction of this molecular form may even evaporate into the cavity (gaseous) region from the gas–liquid interface. Thus, the overall decomposition of *p*-NP at low pH (higher acidic solution) is considered to take place in both the gaseous and interfacial film regions by pyrolysis and free radical attack. On the other hand, if the pH is high (lower acidic concentration) or when it approaches a neutral value, then the amount of ionic form predominates. The ionic form of *p*-NP is non-evaporative. Thus, the amount of diffusion of this ionic species is restricted only into the interfacial film region. Therefore, the decomposition of *p*-NP at higher pH is assumed to occur only in the film region and thus the rate of *p*-NP degradation is reduced. So, the two different forms of *p*-NP species due to the change in pH results into different reaction behaviour during the sonication process.

5.2. Effect of bulk solution temperature

The already reported effect of the bulk solution temperature on the degradation rate is contradictory. Bhatnagar et al. [13] reported that ultrasonic decomposition rate constants of 1,1,1-trichloroethylene were almost constant between −7 and 20 °C. Sehgal and Wang [14] demonstrated that the sonication rate constants of thymine increased with the temperature for experiments conducted above 52 °C, and the rate constants were almost unaffected by the temperature between 30 and 52 °C. Chen and Kalback [15] indicated that the reaction rate constants of methylacetate on sonication increased with the temperature between 30 and 40 °C. Koszalka et al. [16] reported that sonication of tetrachloromethane had higher removals of about 85% between 25 and 35 °C and had lower removals of about 48% between 85 and 95 °C. In order to understand the temperature effects with the application of frequency, the decomposition of *p*-NP was conducted at bulk solution temperatures between 20 and 50 °C for the three frequency modes applied. The results of the first-order degradation of *p*-NP at the bulk liquid temperature of 20 °C (pH 5.0) for the three frequency modes are shown in Fig. 2. Similar trends were obtained at other bulk liquid temperatures of 30, 40 and 50 °C. Influence of these three frequency modes on the effect of bulk liquid temperature to the rate constants is shown in Fig. 4. From the figure it can be found that the rate constant for 25 kHz at 20 °C, $k_{20^\circ} = 1.33 \times 10^{-5}\,s^{-1}$, which then decreased to a value of $k_{30^\circ} = 6.67 \times 10^{-6}\,s^{-1}$ at 30 °C and then to $k_{40^\circ} = 5.0 \times 10^{-6}\,s^{-1}$ at 40 °C and finally to $k_{50^\circ} = 3.33 \times 10^{-6}\,s^{-1}$ at 50 °C.

In the case of 40 kHz frequency, the rate constant at 20 °C is $k_{20^\circ} = 1.67 \times 10^{-5}\,s^{-1}$, which further decreased to a

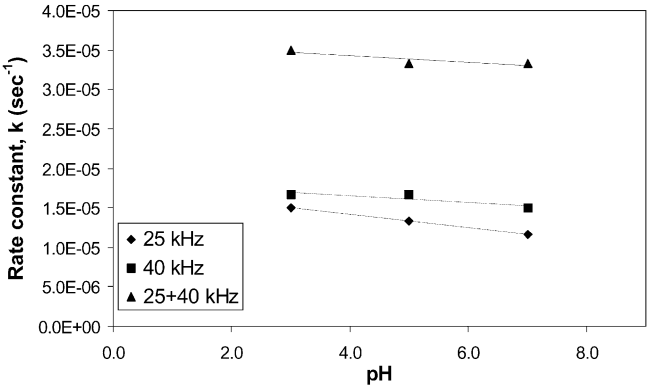

Fig. 3. Effect of pH on the rate constant of *p*-NP degradation for three frequency modes (20 °C, $C_0 \sim 10$ ppm).

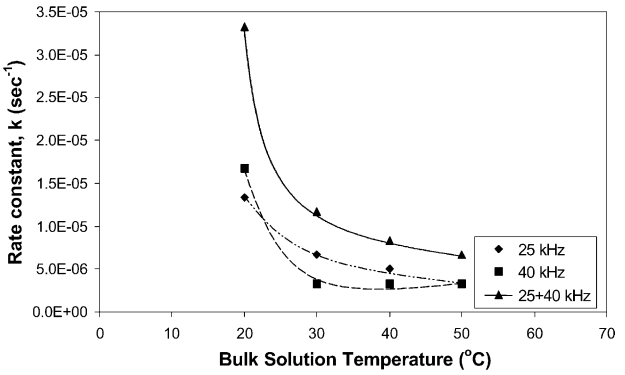

Fig. 4. Effect of bulk solution temperature on the rate constant of *p*-NP degradation for three frequency modes (pH 5.0, $C_0 \sim 10$ ppm).

constant value for the temperatures of 30, 40 and 50 °C, i.e., $k_{30^\circ} = k_{40^\circ} = k_{50^\circ} = 3.33 \times 10^{-6}\,s^{-1}$ or in otherwise between the temperature range 30–50 °C there is no change in the rate constant.

Whereas, for 25 + 40 kHz frequency mode, the rate constants continuously decreased in the range of temperatures studied, i.e., from a value of $k_{20^\circ} = 3.33 \times 10^{-5}\,s^{-1}$ at 20 °C, then to $k_{30^\circ} = 1.17 \times 10^{-5}\,s^{-1}$ at 30 °C, again to $k_{40^\circ} = 8.33 \times 10^{-6}\,s^{-1}$ at 40 °C, and finally to a value of $k_{50^\circ} = 6.67 \times 10^{-6}\,s^{-1}$ at 50 °C.

Thus, in all the three cases increase in the temperature decreases the rate constant or remains independent but this range of temperature is different for different operating frequencies. Decrease in the rate constant with an increase in the temperature is possibly due to the decrease in the surface tension and viscosity of the given solution, so that the generation of bubbles become easier. But, an increase in the temperature results in a dramatic increase in the vapour pressure of the liquid, which results in higher vapour content of the cavitating bubbles. Under these conditions, the maximum temperature and pressure created in such vaporous transient cavitation bubbles have been shown to be much lower [17] or it results into a cavitational collapse of lower intensity [18]. In addition, with an increase in the temperature, there is a continuous degassing of the solution leading to lower gas nuclei for cavitation (lower cavity population) and hence lower rates of reactions. Thus, the observed behaviour of *p*-NP degradation at higher temperatures is consistent with the present theoretical understanding of sonochemistry and possibly indicates the reasons for the different effects of temperature reported in the literature.

Modelling of the cavitation phenomena to study the effect of temperature on the degradation of *p*-NP was carried out using the equations discussed earlier (Eq. (5)). Change in the temperature affects the vapour pressure, density, viscosity and surface tension, thereby resulting in different cavity dynamics. The intensities measured calorimetrically for the three modes of frequencies given earlier were used for the estimation of actual driving pressures (P_A) for different cases and the cavity dynamics studied. Fig. 5 shows R/R_0 vs. time curve for the three frequency modes and it can be observed that there is enhanced bubble growth when a combination (25 + 40 kHz) is used. In the earlier work [19], the experimental observations were related to the cavity collapse pressures or temperatures based on the numerical simulations. The complexities such as liquid phase compressibility effect, the final collapse cavity size consideration, etc., were avoided by using the Rayleigh–Plesset equation and termination step was avoided by relating the observed degradation rates with the factor R_m^3/t_c [19], where R_m is the maximum size reached by the cavity and t_c the time in which the bubble collapses. Tatake and Pandit [19] have also shown that R_m^3/t_c is a good correlating parameter to explain the observed cavitational yields. This is due to that a change in the radius of the bubble will not give a clear idea about the number of radicals generated and hence cannot be related to chemical yields. But, R_m^3/t_c parameter appropriately relates the collapse pressures to changes in the volume as the mass or volume of the cavity indicates the number of reactive radicals produced. The results of the effect of temperature on *p*-NP degradation as a function of R_m^3/t_c are given in Fig. 6. The maximum size reached by the cavity in the case of 25 + 40 kHz ($61.86R_0$) is 50% more than 25 kHz ($40.67R_0$) alone and three times more than 40 kHz ($15.6R_0$). Also, the intensity in the case of 25 + 40 kHz (0.39 W/cm^2) combination is nearly same as that for 40 kHz (0.36 W/cm^2) wave and less than that for 25 kHz (0.46 W/cm^2). Thus the simulations indicate that due to a dual frequency combination there is enhanced bubble growth for nearly same overall intensities as that for single frequency, which ultimately results in higher degradation and again a correspondence between the degradation and the parameter R_m^3/t_c has been established.

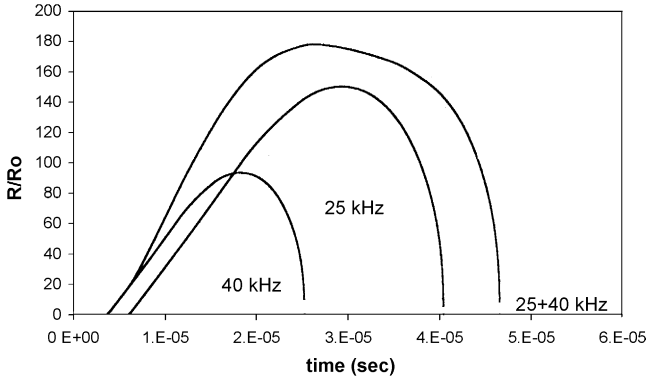

Fig. 5. Plot for R/R_0 vs. time for three frequency modes.

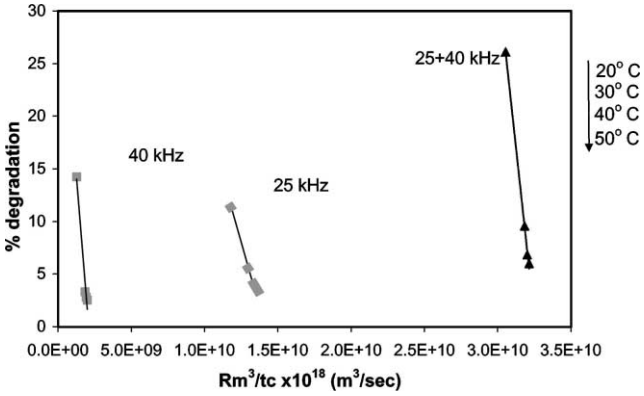

Fig. 6. Effect of temperature on *p*-NP degradation as a function of R_m^3/t_c.

5.3. Effect of initial concentration

The effect of concentration on *p*-NP degradation was studied for the initial concentrations of 10, 100 and 500 ppm (pH 5.0, temperature 20 °C) for the three frequency modes. Fig. 7 depicts the effect of initial concentration on the rate constant of *p*-NP degradation for the three frequency modes.

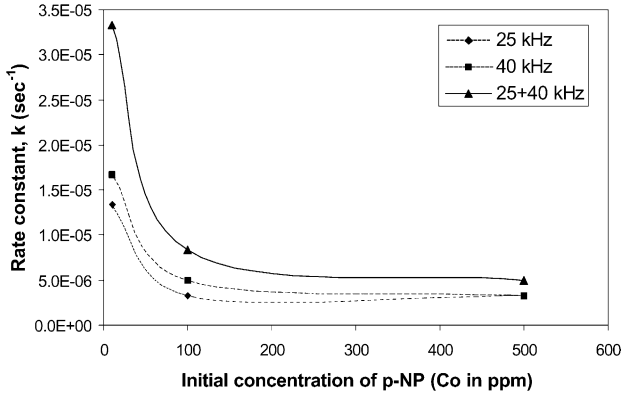

Fig. 7. Effect of initial concentration (C_0) on the rate constant of *p*-NP degradation for three frequency modes (pH 5.0, 20 °C).

While *p*-NP degraded exponentially with respect to time irrespective of the initial concentration, the rate was dependent on the initial concentration of *p*-NP. In the case of 25 kHz frequency, the apparent first-order rate constant decreased from $1.33 \times 10^{-5}\,s^{-1}$ for a $(p\text{-NP})_i$ of 10 ppm to a value of $0.33 \times 10^{-5}\,s^{-1}$ for a $(p\text{-NP})_i$ of 100 ppm and after this the rate constant was unchanged even when the initial concentration was increased to 500 ppm. Whereas, for 40 and 25 + 40 kHz frequencies, even though a similar trend of decrease in rate constant was observed, it decreased even when the initial concentration was changed from 100 to 500 ppm and the resulting change was still a significant one. It was 34% decrease for 40 kHz and 40% for 25 + 40 kHz when it was changed from 100 to 500 ppm. Also, from the above results it could be interpreted that at lower initial concentration, the rate limiting step was considered to be the diffusion of *p*-NP into the interfacial film region (reaction zone). In this region, the reaction between *p*-NP and free radicals was assumed to occur very fast. Thus, at lower initial *p*-NP concentration, the overall *p*-NP degradation is controlled by diffusion and the mass diffusion rate is linearly dependent on the concentration of *p*-NP in the bulk liquid surrounding the film region (driving force, $C_b - C_I$, C_b is the concentration of *p*-NP in the bulk and C_I the concentration of *p*-NP in the film region). Alternatively, at higher initial *p*-NP concentration, this diffusion limitation is absent. The above mechanism is correct only if the free radical concentration is low in the interfacial region. Thus, in the case where the initial *p*-NP concentration in the bulk is low, these available *p*-NP are sufficient to consume the available free radicals resulting in higher rates. However, when the initial *p*-NP concentration is high and diffusion limitation is absent, yet the rates are lower as they are controlled by the low concentration of free radicals. This has been conclusively established with the observed experimental results. Thus, the degradation mechanism of *p*-NP appears to shift from substrate controlled (at lower initial *p*-NP concentration) to free radical controlled (at higher initial *p*-NP concentration).

The overall degradation efficiency of *p*-NP depends on the number of hydroxyl radicals generated as well as on the rate with which they are released into the surrounding medium. In our case, we have tried to relate this phenomenon to the collapse time of a single cavity. If the cavity collapses faster, the rate of release of these radicals into the medium is higher. A cavity driven at 40 kHz collapses faster (3.02 μs) as compared to a cavity driven at 25 kHz (5.68 μs) or 25 + 40 kHz (7.75 μs). Hence the release of radicals into the medium is faster at 40 kHz as compared to at 25 or 25 + 40 kHz. But, from the experimental results, it was observed that for 40 kHz, the rate of degradation is not higher as compared to 25 kHz. This clearly indicates that the degradation rate is not only a function of rate of release, but also depends on the number of available radicals in the medium.

This may be due to that the number of cavities generated at 40 kHz is not as high as at 25 kHz, as the intensity of 40 kHz wave is less than that of 25 kHz wave and also it is known that the cavitational threshold intensity is higher at higher frequency resulting into lower cavity population at higher frequency. Of course these modelling studies are not rigorous, as there is no clear information about the number of bubbles in the given medium of cavitation. Efforts are being made to find out the number of radicals and incorporate the same to get the complete picture.

5.4. The effect of dissolved gases

Wakeford et al. [20] have found out that the yield of H_2O_2 increases by six times for an air saturated solution than for N_2 saturated solution, which in turn was responsible for the higher rates of reactions carried out under the atmosphere of air. In the present study, reactions were also carried out in the absence of air for 25 kHz (pH 5.0 and 7.0). Also, for 40 kHz, reactions were carried out in presence of nitrogen as well as in absence of air at a pH 5.0. The obtained experimental observations have been shown in Fig. 8.

The rate constant in the presence of air at pH = 5.0 for 25 kHz frequency mode, i.e., $k_{air,25} = 1.33 \times 10^{-5}\,s^{-1}$ and the rate constant at the same pH but in the absence of air is $k_{no\,air,25} = 1.17 \times 10^{-5}\,s^{-1}$. Also, for the same frequency application at pH 7.0 the rate constant in the presence of air is lower than at pH 5.0. But, at a pH 7.0 with the presence of air and at a pH 5.0 in the absence of air show the same rate constants, i.e., $k_{air,25} = k_{no\,air,25} = 1.17 \times 10^{-5}\,s^{-1}$, but degradation in each of these cases is marginally different from each other. (In the absence of air for pH = 5.0, the degradation is about 9.88% and in the presence of air the degradation is about 11.36%. At pH = 7.0, in the absence of air the degradation is 9.83%, whereas it is about 10.16% in the presence of air.)

Also, from Fig. 8 it could be seen that in the presence of air and nitrogen purging for 40 kHz frequency application indicate that decomposition increases more with air saturated solution than for nitrogen. This can be seen from the rate constants obtained in the presence of air, $k_{air,40} =$

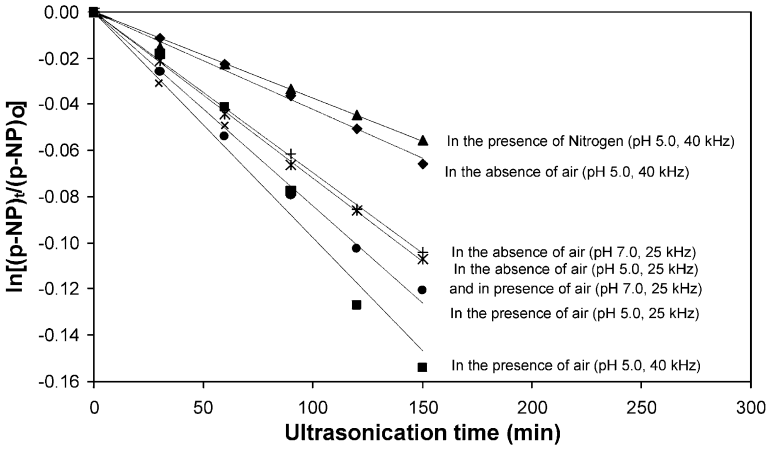

Fig. 8. Effect of gas atmosphere (air or nitrogen) on the first-order degradation of *p*-NP using 25 and 40 kHz (pH 5.0 and 7.0, 20 °C, $C_0 \sim 10$ ppm).

$1.67 \times 10^{-5}\,s^{-1}$, whereas in the presence of nitrogen it is $k_{\text{nitrogen},40} = 0.67 \times 10^{-5}\,s^{-1}$. Thus, there is approximately twofold increase in the rate constant in the presence of air. The presence of dissolved oxygen in aqueous solution has been reported to play a very important role on the generation of highly oxidative hydroxyl and hydroperoxyl free radicals [12,21], and these radicals might enhance the decomposition of *p*-NP. On the contrary, dissolved nitrogen present in aqueous solution might scavenge the free radicals [12] and inhibit the free radical attack on *p*-NP. Therefore, the free radical attack in both the gaseous and interfacial film regions are strongly influenced by the dissolved gases present in the aqueous solution. The decomposition of *p*-NP by pyrolysis mechanism is supposed to be independent of the oxygen and nitrogen gases purged into the sonication reactor because the polytropic index (C_p/C_v) of oxygen and nitrogen is almost the same, i.e., 1.39 for oxygen and 1.40 for nitrogen [17]. Therefore, the temperatures of gaseous and film regions are relatively constant despite the variation in the presence of gases. Even though, the rate constant in the absence of air is the same as that of nitrogen ($k_{\text{no air},40} = 0.67 \times 10^{-5}\,s^{-1}$), but the percentage degradation for the *p*-NP solution in the absence of air is marginally higher than for nitrogen saturated solution (degradation in the absence of air is 6.34%, whereas in the presence of nitrogen it is 5.41%). This also suggests that pyrolytic reaction has a much lower contribution to the overall degradation rate and the reaction is essentially controlled by the generation and availability of the free radicals.

5.5. Effect of ultrasound energy dissipation area

In order to understand the effect of emitter area or the dissipation area on the degradation rate, the reaction was conducted using an ultrasonic horn (22.5 kHz, 240 W) with different area of emitter tips. The experimental results of using different emitter area of horn (using 100 ml volume) on the first-order degradation of *p*-NP are shown in Fig. 9. When

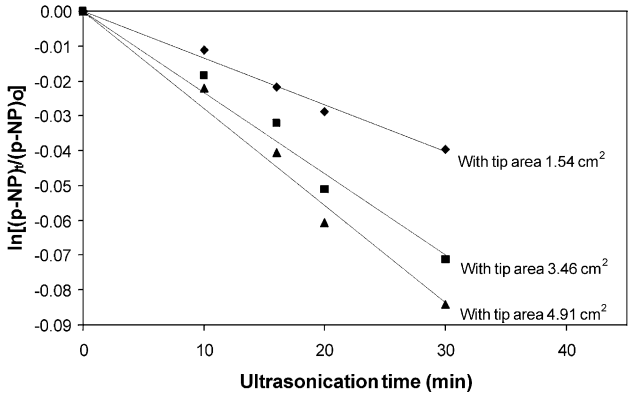

Fig. 9. First-order plot for *p*-NP degradation using different emitter area of horn (pH 5.0, $C_0 \sim 10$ ppm, 20 °C).

the power intensity associated with ultrasound was changed from 4.31 to 5.27 W/cm^2 and then to 7.93 W/cm^2 (by using emitting tip areas of 4.9, 3.46 and 1.54 cm^2, respectively), the percentage degradation and hence the rate constants also decreased. This may be due to the fact that for the same energy input, if the area of the emitting surface is decreased, it results in delivering of much higher intensity (W/cm^2). This increase in intensity causes an increase in number of bubbles formed close to the emitting surface. Due to this increase, the formed bubbles coalesce resulting in larger bubbles, which cannot violently cavitate anymore affecting the formation of free radicals and thereby resulting in lower energy efficiency [22]. Alternatively, with lower intensity (higher dissipation area) the reaction rates are higher due to a better distribution of the supplied energy. Also, with an increase in intensity, there is a possibility of decoupling between the emitter surface and the solution, which affects the net cavitational efficiency [23]. Again, bubble shroud formation may occur at the surface of the emitter at higher intensities resulting in attenuation of sound pressure levels.

Simulations were again carried out for different intensities of the horn (by using different emitter tips). Using the

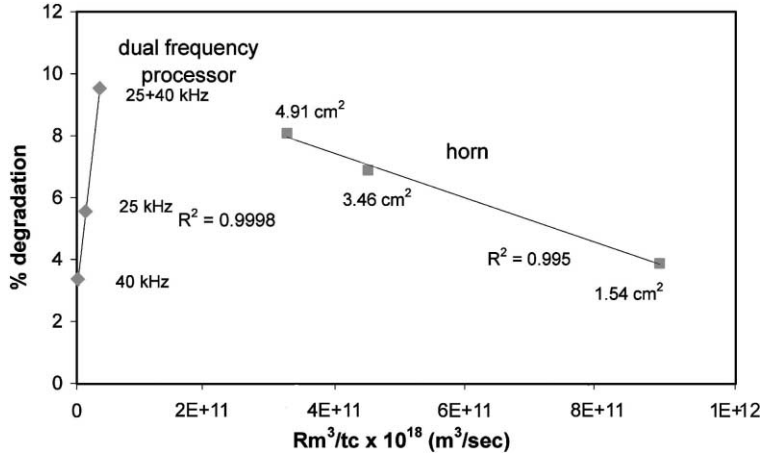

Fig. 10. Plot for *p*-NP degradation (%) vs. R_m^3/t_c for dual frequency processor and horn (20 °C).

modelling results of these two acoustic equipments (horn and dual frequency processor), the observed degradation rates with the factor R_m^3/t_c can be related and are plotted as shown in Fig. 10.

From the plot it can be seen that the trends observed in the case of horn is exactly opposite to that of dual frequency processor. In the case of dual frequency processor, the degradation rates were found to increase with an increase in the intensity. Entezari and Kruus [24] reported that for KI decomposition, which proceeds via a free radical mechanism, an increase in intensity results in an increase in the KI decomposition rates up to an optimum value of intensity after which it decreases. But in the present case, the intensity could be more than the optimum, thus showing the continuous downward trend (in the case of horn).

Also, as compared to a dual frequency acoustic processor the intensity is very high for the horn, but there is no proportionate increase in the rates of degradation. This could be due to (1) operating the horn at higher intensities than optimum, and (2) due to the nature of the acoustic field generated which may be different from that of dual frequency acoustic processor. Standing waves are formed in an ultrasonic horn due to the reflection of the waves from the base as well as from the sides of the reactor decreasing the energy efficiency of the same. This problem is overcome in the dual frequency acoustic processor in which the interference pattern formed due to the two opposing waves disturb the standing wave pattern resulting in the higher energy efficiencies [6].

5.6. Effect of the acoustic field generated

As can be seen from the studies of horn and dual frequency acoustic processor, the degradation rates are not increasing proportionately with intensity for horn as compared to dual frequency acoustic processor. This could be due to the difference in the nature of the acoustic field generated. In order to understand this in detail, studies were carried out in an ultrasonic bath (Dakshin, 22.5 kHz, 120 W) with the volume of 500 ml and dissipation area of 225 cm^2. It has been found out from the first-order plot, the rate constant of the reaction is $1.67 \times 10^{-5}\,s^{-1}$. The intensity of bath (based on calorimetric measurements, 0.18 W/cm^2) is approximately 24 times less than that of horn (4.31 W/cm^2) and two times less than that of dual frequency processor (0.88 W/cm^2). But, the observed degradation rates do not vary directly with the variation in the intensity. The degradation in bath is 13.67%, which is half of that obtained in the case of dual frequency acoustic processor (26.1%) operating with 25 + 40 kHz. This variation could be due to the difference in the nature of the acoustic field present in these equipments. The change in frequency and intensity of ultrasonic waves changes the dynamics of the cavity. Though the change in frequency and intensity is incorporated in the cavity dynamics, all the points for all the combinations do not lie on a straight line (Fig. 10). But, for a given equipment the points indeed lie on a straight line.

This suggests that the variation is due to the difference in the acoustic field generated in these equipments and also possibly due to the variation in the cavity population. Also, one point should be considered that the volume of the

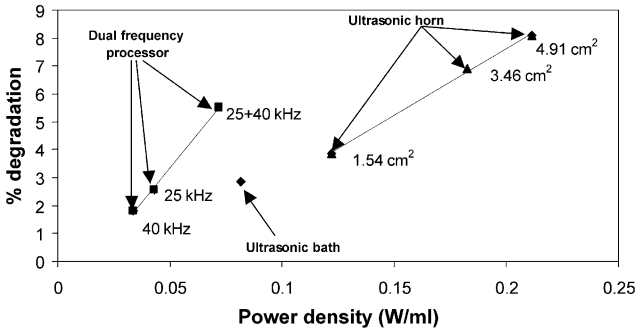

Fig. 11. Plot for power density with percentage degradation (for 30 min operation).

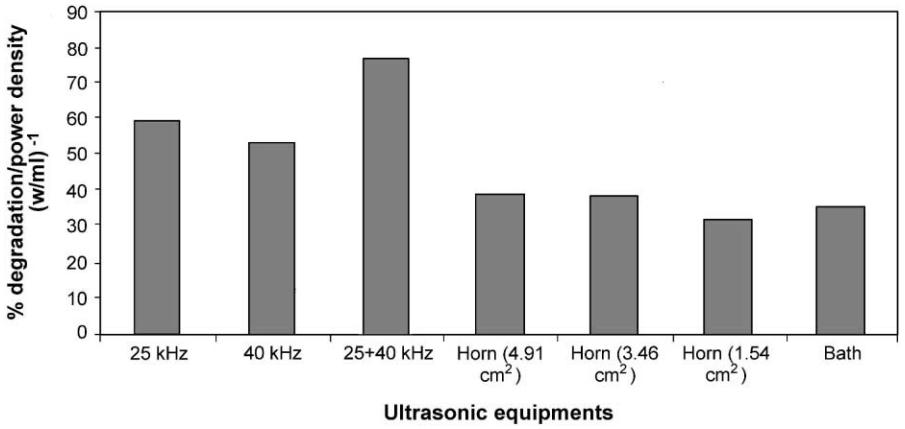

Fig. 12. Effect of percentage degradation/power density for various ultrasonic equipments.

solution taken in all these equipments is not the same. Thus, we can consider the power dissipated per unit volume of the solution, i.e., power density.

5.7. Comparison based on power density

In any ultrasonic transformation study, the power should be optimised, even when the chemical evolution of the system seems simple. In general, the sonication should not be automatically turned to a maximum power. Because, at sufficiently high power, there is no further increase in the reaction rate as reported in the literature [3,25]. Thus, optimisation with power, i.e., with power density as a possible parameter becomes crucial as this parameter directly gives an idea about the amount of energy dissipated in a given volume of the solution. Fig. 11 plots the results of the experimental observations made with dual frequency set-up, ultrasonic horn and a bath. Based on power density, the observed degradation rates cannot be directly correlated for all the systems though the general trend is an increase in the yield with an increase in power density. From the graph, it is clear that for the nearly same power density, the degradation for dual frequency processor is approximately twice than that obtained in bath. Also, when compared with the horn, the power density of dual frequency processor is lower by six times, but the degradation is almost the same in horn and dual frequency processor. Hence, even though power supplied to the system is same, the extent of degradation varies. This fact also emerges clearly if one compares the results of horn with different dissipating areas. This is therefore due to the difference in the nature of the acoustic field and possibly due to the variation in intensity as well. The dual frequency acoustic processor ($25 + 40$ kHz) is more energy efficient than the bath, as for the same power density (W/ml) the degradation is approximately twice.

Also, for a given equipment power density is a good parameter to understand the effect of varying energy supplied to the system and to optimise the same. The energy required to expand a population of bubbles in solution can be estimated with the following equation:

$$E = (\tfrac{4}{3})R_{\mathrm{m}}^3 PN \tag{7}$$

where R_{m} is the maximum radius of the bubble before it collapses, P the magnitude of the hydrostatic and acoustic pressure, and N the number of bubbles in solution.

This equation again confirms that number of bubbles will increase linearly with power density. Although, the number of chemical events per bubble is not known, it is reasonable to expect a linear correlation of chemical reactivity with the amount of energy transferred into the solution. But this equation fails to explain the observed effects in the case of horn. This may be due to the occurrence of decoupling because of high intensities of ultrasound associated with the horn.

For any equipment the energy efficiency can be defined as the observed output divided by the power input or in the present case the amount of *p*-NP degraded to the power supplied per unit volume (power density). Fig. 12 is a plot of percentage degradation/power density for various equipments studied. From the plot, we could observe that percentage degradation/power density value is maximum for the dual frequency processor. As compared to 25 and 40 kHz the efficiency for the 40 kHz set-up is enhanced when operated along with the 25 kHz wave. This suggests that the efficiency of the reactor is enhanced when operated together (i.e. in a dual frequency mode).

Also in the case of horn the efficiency decreases when operated above a specific intensity. This suggests that there exists an optimum intensity for which the degradation is maximum.

6. Conclusions

The application of ultrasound for the control of oxidisable trace contaminants in water has the potential to become a

competitive technology as compared to other methods of oxidation. Although, the information presented here is the result of only a preliminary study we feel justified in drawing the following conclusions:

1. From the experiments, it has been established that to get higher degradation of *p*-NP, irrespective of the application of the frequency mode, it is better to operate at lower pH (at least at 5.0) with the passage of air and keeping the temperature of the bulk solution as minimum as possible (20–30 °C).
2. The effect of initial concentration of the pollutant indicates that it is better to operate at lower initial concentration but not lower than the hydroxyl radicals production rate as it will waste the usefulness of the radicals produced. Above all, the dissipation area becomes an important parameter as it has been observed from the study that increasing the area for the same energy input increases the rate of the degradation up to an optimum above which it decreases.
3. By operating both the frequencies simultaneously, the rate of the reaction is more than their combined individual effects. Francony and Petrier [26] have reported an increase in the degradation with an increase in ultrasonic frequency. But, in their studies they have used frequency ranges from 20 to 1078 kHz. So, we can expect an altogether a different behaviour once the frequency is changed to a higher value from the lower one due to the change in the dynamics of the bubble. But, in our study, the applied frequency ranges are very close (25, 40 and $25+40$ kHz), still it resulted in larger rate constants. The reason for this behaviour has been explained on the basis of the simulations of the bubble dynamics behaviour.
4. Although, the absolute contributions of the potential rate enhancement explanations will be difficult to establish, at least at this stage, these results give an idea about the dual frequency effects on the given chemical reaction under various controllable external parameters. Thus, further experimentation will determine their relative importance in order to predict and optimise design and performance characteristics. Further work aimed at elucidating the optimal distance (gapwidth) between the two plates for a dual frequency processor. This could result in higher sonochemical efficiency and hence higher reaction rates for a given energy input. From the above results, application of this dual frequency technique appears to be a suitable alternative as compared to just increase in ultrasonic power operating with single frequency. More efforts are being made to quantify the nature of the acoustic field present in different types of ultrasonic equipments.
5. In the case of horn it has been observed that increase in intensities did not result in higher degradation rates. Also, the model developed could not explain the observed effects due to the possibility of decoupling of the ultrasound at higher intensities as reported in the literature [23].

The major contribution of this paper is to link a rather complete cavity dynamics model with degradation rates of *p*-NP with a parameter R_m^3/t_c and show its usefulness in correlating cavitational yield. With such a model it has been possible to obtain some trends concerning the effects of initial pollutant concentration, temperature and ultrasonic energy dissipation area which are in good agreement with experimental results.

References

[1] A. Kotronarou, G. Mills, M.R. Hoffmann, J. Phys. Chem. 95 (1991) 3630–3638.
[2] K.S. Suslick, Sci. Am. 260 (1989) 80–86.
[3] I. Hua, R.H. Hochemer, M.R. Hoffmann, Environ. Sci. Technol. 29 (1995) 2790–2796.
[4] A. Kotronarou, G. Mills, M.R. Hoffmann, Environ. Sci. Technol. 26 (1992) 1460–1462.
[5] D.L. Currell, G. Wilheim, S. Nagy, J. Am. Chem. Soc. 85 (1963) 127–130.
[6] P.A. Tatake, A.B. Pandit, Chem. Eng. Sci., submitted for publication.
[7] G. Thoma, J. Swofford, V. Popov, M. Som, Adv. Environ. Res. 1 (1997) 178–193.
[8] M.S. Plesset, A. Prosperetti, Ann. Rev. Fluid Mech. 9 (1977) 179.
[9] D.V. Prasadnaidu, R. Rajan, R. Kumar, K.S. Gandhi, V.H. Arakeri, S. Chandrasekaran, Chem. Eng. Sci. 49 (1994) 877–888.
[10] S. Okouchi, O. Nojima, T. Arai, Wat. Sci. Technol. 26 (1992) 2053–2056.
[11] Y. Ku, K.Y. Chen, K.C. Lee, Wat. Res. 31 (1997) 929–935.
[12] J.M. Wu, H.S. Huang, C.D. Livengood, Environ. Prog. 11 (1992) 195–201.
[13] A. Bhatnagar, S. Kurup, A. Brenner, H.M. Cheung, J.J. Wong, Paper Presented at the AIChE Summer National Meeting, Minneapolis, MN, 1992.
[14] C.M. Sehgal, S.Y. Wang, J. Am. Chem. Soc. 103 (1981) 6606–6611.
[15] J.W. Chen, W.M. Kalback, Ind. Eng. Chem. Fund. 6 (1967) 175–178.
[16] D.P. Koszalka, J.F. Soodsma, R.A. Bever, Paper Presented at the AIChE Summer National Meeting, Minneapolis, MN, 1992.
[17] T.J. Mason, J.P. Lorimer, Sonochemistry: Theory, Applications and Uses of Ultrasound in Chemistry, Ellis Horwood, Chichester, UK, 1998.
[18] K.S. Suslick, Ultrasound: Its Chemical, Physical and Biological Effects, VCH, New York, 1988.
[19] P.R. Gogate, P.A. Tatake, P.M. Kanthale, A.B. Pandit, AIChE J., submitted for publication.
[20] C.A. Wakeford, R. Blackburn, P.D. Lickiss, Ultrason. Sonochem. 6 (1999) 141–148.
[21] N. Serpone, R. Terzian, H. Hidaka, E. Pelizzetti, J. Phys. Chem. 98 (1994) 2634–2640.
[22] A. Henglein, M. Gutierrez, J. Phys. Chem. 94 (1990) 5169–5172.
[23] B. Ondruschka, J. Lifka, J. Hofmann, Chem. Eng. Technol. 23 (2000) 588–592.
[24] M.H. Entezari, P. Kruus, Ultrason. Sonochem. 3 (1996) 19–24.
[25] M. Sivakumar, A.B. Pandit, Ultrason. Sonochem. 8 (2001) 233–240.
[26] A. Francony, C. Petrier, Ultrason. Sonochem. 3 (1996) S77–S82.